

Topical Report

**ADVERSE EFFECTS OF MINERAL-ALKALI REACTIONS IN ALKALINE FLOODING:
A REAPPRAISAL**

Project BE4B, FY89

By P. B. Lorenz

Jerry Casteel, Project Manager
Bartlesville Project Office
U. S. Department of Energy

Work Performed for the
U. S. Department of Energy
Under Cooperative Agreement
DE-FC22-83FE60149

DISCLAIMER

This report was prepared as an account of work sponsored by an agency of the United States Government. Neither the United States Government nor any agency thereof, nor any of their employees, makes any warranty, express or implied, or assumes any legal liability or responsibility for the accuracy, completeness, or usefulness of any information, apparatus, product, or process disclosed, or represents that its use would not infringe privately owned rights. Reference herein to any specific commercial product, process, or service by trade name, trademark, manufacturer, or otherwise, does not necessarily constitute or imply its endorsement, recommendation, or favoring by the United States Government or any agency thereof. The views and opinions of authors expressed herein do not necessarily state or reflect those of the United States Government or any agency thereof.

IIT Research Institute
National Institute for Petroleum and Energy Research
P. O. Box 2128
Bartlesville, Oklahoma 74005
(918) 336-2400

PREFACE

An examination of the results presented in NIPER Report No. 273 showed that further interpretation was needed, and the present report is based on a new analysis of the data. This constitutes an extra report, not part of the milestone schedule. Some new conclusions are drawn, and some conjectures are proposed that suggest further experiments. The most important conclusion is that the data confirm the effectiveness of low-pH surfactant-enhanced alkaline flooding.

For a description of the experimental procedures, consult the original report. Tables and illustrations that contain data used in the new analysis are reproduced in this report. Figures 2A and 14A are modified versions of figures 2 and 14. This report gives a textual description of the experimental results, which was incomplete in the original report. The differences in interpretation from those in NIPER-273 are primarily a result of emphasizing different data.

TABLE OF CONTENTS

	<u>Page</u>
Preface.....	ii
Abstract.....	1
Bottle Tests.....	1
Experimental Results.....	1
Interpretation.....	2
Slim Tubes: Results and Interpretation.....	2
Alkalinity.....	2
Sodium and Potassium.....	4
The Divalent Cations.....	5
Silicon and Aluminum.....	6
Comparison of Bottle and Slim Tube Tests.....	7
Summary and Conclusions.....	8
References.....	10

NOTE: Tables and illustrations are reproduced from NIPER-273 for ready reference. Those not explicitly discussed are omitted.

TABLES

1.-4.....	Not reproduced
5. Results of bottle test with Gu-Dao sandstone and 0.5 N NaOH solution at 60° C.	11
6. Results of bottle test with Gu-Dao sandstone and 0.5 N Na ₂ SiO ₃ solution at 60° C.	11
7. Results of bottle test with Gu-Dao sandstone and 0.5 N Na ₂ SiO ₃ solution at 60° C. solution).....	12
8. Results of bottle test with Liao-He sandstone and 0.5 N NaOH solution at 60° C.	12
9. Results of bottle test with Liao-He sandstone and 0.5 N Na ₂ SiO ₃ solution at 60° C.	13
10. Results of bottle test with Liao-He sandstone and 0.5 N Na ₂ CO ₃ solution at 60° C.	13

TABLES--Continued

	<u>Page</u>
11. Consumption of alkali in slim tube experiments.....	14
12. Effluent profile for alkalinity in the slim tube experiment with Gu-Dao sandstone and 0.5 N NaOH solution.	14
13. Effluent profile for alkalinity in the slim-tube experiment with Liao-He sandstone and 0.5 N Na ₂ CO ₃ solution.	15
14. Silicon, aluminum, and potassium in the effluent from Liao-He sandstone during injection of 0.5 N Na ₂ CO ₃ solution at 60° C.....	16
15. Parameters used in calculation of saturation indices for calcite and chrysotile - 60° C.....	17
16.-17.....	Not reproduced
18. Parameters used for calculation of carbon speciation.	17
19.-20.....	Not reproduced

ILLUSTRATIONS

1. Effluent profile for alkalinity in the Gu-Dao/NaOH slim-tube experiment.....	18
2A. Effluent profile for alkalinity in the Liao-He/Na ₂ CO ₃ slim-tube experiment.....	19
3. Effluent profile for the tracer, bromide ion, in the Liao-He/Na ₂ CO ₃ slim-tube experiment.....	20
4. Effluent profiles for sodium (Na) and potassium (K) in the Gu-Dao/NaOH slim-tube experiment.....	21
5. Effluent profile for sodium (Na) in the Liao-He/Na ₂ CO ₃ slim-tube experiment.....	22
6.....	Not reproduced
7. Concentration of sodium (Na) and alkalinity versus time in the Liao-He/Na ₂ CO ₃ bottle test.....	23
8. Effluent profiles for calcium (Ca), magnesium (Mg), and aluminate ion (Al) in the Gu-Dao/NaOH slim-tube experiment.....	24
9. Effluent profiles for calcium (Ca) and magnesium (Mg) in the Liao-He/Na ₂ CO ₃ slim-tube experiment.....	25

ILLUSTRATIONS--Continued

	<u>Page</u>
10. Effluent profile for silicate ion (Si) in the Gu-Dao/NaOH slim-tube experiment.....	26
11. Concentrations of silicate ion (Si) and aluminate ion (Al) versus time in the Gu-Dao/NaOH bottle test.....	27
12. Concentrations of silicate ion (Si) and aluminate ion (Al) versus time in the Liao-He/Na ₂ CO ₃ bottle test.....	28
13.....	Not reproduced
14A. Ideal pH values for neutralization of carbonate and bicarbonate solutions.....	29

ADVERSE EFFECTS OF MINERAL-ALKALI REACTIONS IN ALKALINE FLOODING:

A REAPPRAISAL

By P. B. Lorenz

ABSTRACT

An analysis is presented of data from experiments on mineral-alkali reactions. The most informative experiments consisted of injection into "slim tubes" containing crushed sand: (I) NaOH into a high-clay sand, and (II) Na₂CO₃ into a low-clay sand. A fast (ion exchange) reaction occurred in both experiments, consuming 42% and 4% of the alkalinity in a 1-PV slug, respectively for I and II. A slow (dissolution-precipitation) reaction consumed about the same proportions, but ceased in II and continued indefinitely in I. Peaks of sodium, calcium, and magnesium concentrations in the effluent of I prior to expected breakthrough are unexplained, but may be partly associated with pre-saturation with KCl and the presence of K-feldspar. Relative timing of Si and Al effluent profiles suggest two precipitation reactions with different Al/Si stoichiometry. Onset of precipitation appears to be delayed by a lag in nucleation. The failure of simple equilibrium calculations to account for alkalinity, pH, and concentrations of calcium and carbonate in the effluent from II indicates complex equilibria or slow kinetics.

Results were generally confirmed by bottle tests, but there was more dissolution-precipitation activity with the system of I, probably because pH remained high at the higher liquid/solid ratio.

BOTTLE TESTS

Experimental Results

The data resulting from bottle tests¹ show a small initial discrepancy between alkalinity and sodium (tables 5 to 10), and small unexpected increases in both for the reaction of LH sand* with sodium carbonate. This indicates experimental errors, or minor extraneous phenomena, and it is therefore inappropriate to draw conclusions about alkali consumption from small

*For convenience, Liao-He will be abbreviated LH, and Gu-Dao will be abbreviated GD.

changes. The clear-cut trends in the data are that there was a slow decline in alkalinity of sodium hydroxide and sodium silicate solutions in the presence of both sands, and the decline showed every sign of continuing past 170 hr. There was a parallel decline in sodium concentration with GD, but the sodium data for LH were somewhat ambiguous. The apparent spike in sodium concentration at 9 hr in the experiment with NaOH (table 8) represents a production of 0.004 equivalent, or 0.1 equiv/(kg of sand); this has no obvious explanation.

The data with sodium carbonate solutions are inconclusive. They do not contradict the expected decline in alkalinity with GD sand, but they do not support it definitively. In the bottle tests with Na_2SiO_3 (tables 6 and 9), the initial stoichiometric discrepancy between sodium and silicon* concentrations is probably inherent in the sample of sodium silicate, rather than representing an immediate jump in silicate concentration. There was a steady increase in silicon (which probably would have continued past 170 hr in most cases) with both sands and all three agents. Aluminum* concentration went through a small maximum and returned to zero with both sands and all three agents.

Interpretation

All of the produced chemical species indicated that the reactivity of the three chemicals with reservoir rock decreased, as expected, in the order $\text{OH}^- > \text{SiO}_3^{=} > \text{CO}_3^{=}$, and that the GD sand was more vulnerable than the LH, probably because of its high montmorillonite content. The primary mechanism of alkali consumption was precipitation of sodium aluminosilicate (after dissolution of quartz and clay). The measurements were not designed to detect ion exchange or any possible reaction of strong alkali with calcareous cement.

SLIM TUBES: RESULTS AND INTERPRETATION

Alkalinity

The GD sand with sodium hydroxide (worst case) (fig. 1) had a continuing and unacceptable level of alkali consumption. Because the effluent reached a

*The expressions "silicate concentration" and "aluminum concentration" refer to the total amount of the element in solution, regardless of the ionic species.

plateau at 80% of injected alkalinity, the "consumption of alkali" (table 11) depends on the amount of injected, and does not have any general significance. For a 1-PV slug, the slow reaction would consume 0.055 equiv/kg; i.e., 0.028 equiv., or 44% of the alkali injected.

The LH sand with weak alkali (best case) (fig. 2A) displayed a smaller consumption, which appeared to terminate after 2.5 PV. The actual loss should be derived by subtraction from the dispersion curve in the absence of consumption, as illustrated in figure 2A. The upper end of the dispersion curve is assumed to be the same shape as the lower end. In practice, most curves have an unsymmetrical tail (cf. fig. 3), which would make the estimated loss smaller. From figure 2A, the loss from 1.0 to 2.5 PV is 0.0048 equiv., which is 6% of the 0.080 equivalent injected.

Since "fast" reactions cause chromatographic delay, the magnitude of a fast reaction should be estimated from the displacement of the midpoint of produced alkalinity curve. The calculations are tabulated here:

	<u>GD/NaOH</u>	<u>LH/Na₂CO₃</u>
PV, cm ³	127	106
Alkali injected per PV, equiv.....	0.064	0.053
Chromatographic delay, PV.....	0.42	0.038
Alkali consumed, equiv.....	0.027	0.0020
Weight of sand, kg.....	0.51	0.50
Ion exchange, meq/kg.....	53	4.0

If we assume surface areas of 10 and 1 m²/g for GD and LH, respectively, this consumption amounts to about 1 ion per 25 Å,² which is reasonable for ion exchange.

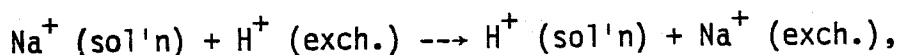
Even after the effluent from the LH sand essentially matched the injected fluid in alkalinity, the effluent pH was 1.2 units lower (table 13). This is puzzling: Figure 14A indicates that at pH 10.1, the CO₃⁼ ion should be 14% converted to HCO₃⁻ (7% neutralization). Figure 14A shows the individual reactions (in the absence of oil) calculated from the equilibrium quotients of table 18, where $Q_1 = [H^+][HCO_3^-]/[CO_2]_{aq}$ and $Q_2 = [H^+][CO_3^{=}] / [HCO_3^-]$. The pH and alkalinity should be related by these standard curves.

One possible cause for the discrepancy would be the replacement of carbonate ions by other bases, which would modify the curves of figure 14A. However, table 10 shows that the most probable bases reach only minor concentrations. Other explanations that could be tested by further experiment are:

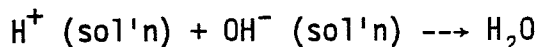
1. The formation of complexes such as NaCO_3^- and CaHCO_3^+ . Conductivity measurements could be used to indicate the presence of such ions.
2. Slow kinetics or metastable equilibria. Such phenomena have been observed in carbonate systems when supersaturated solutions of CaCO_3 persist for a long time.² This could be verified under the present experimental conditions by titrating the sodium carbonate solution with an acid, a soluble calcium salt, and/or a slurry of well-characterized calcium kaolinite.

Sodium and Potassium

With the GD sand, the data at 0.2 PV (Fig. 4) show unexpectedly high sodium and low potassium concentrations. The potassium concentration is only 0.35 of that in the saturating solution, even though the displacement front is still 0.3 PV short of reaching the effluent end. The concentration of sodium corresponds with 16% of that present in the feldspar and may have been displaced by the KCl treatment. The potassium concentration indicates a net loss of 0.082 mol, of which 0.028 mol was presumably consumed by reaction with the sodium feldspar. Apparently 0.054 mol was taken up by the 71 g of non-kaolinitic clay. This is too high to be accounted for by ion exchange. It corresponds with 1 potassium-ion for each 5 unit cells and may have been absorbed by intercalation. The increase in sodium at 0.5 PV is to be expected because this corresponds with the expected arrival of the NaCl front. The dip in sodium concentration at about 1.0 PV is an interruption of the expected rise and can plausibly be attributed to a "fast" reaction, such as ion exchange:



driven by the reaction



The dip corresponds with a deficiency of about 0.02 mol, of the same order of magnitude as that calculated from chromatographic delay. In figure 5, the LH sand shows the same effect.

After alkali breakthrough (1.5 PV), the sodium and alkali effluent profiles are very similar and must represent the same slow reaction, which continues indefinitely. The dip at 2.5 PV and the subsequent plateau are discussed below in connection with the data on silicon and aluminum. The continuing production of potassium suggests a slow reaction of hydroxide with the K-feldspar (table 3). The relative magnitudes of sodium consumption and potassium production indicate that the former is a faster "slow" reaction. Thus clays (especially kaolinite) are more reactive than feldspars.

No slow sodium-consuming reaction of sodium carbonate with LH sand (fig. 5) was detected.

The Divalent Cations

A broad view of the results on effluent calcium and magnesium confirms the expectation that high concentrations of OH^- or $\text{CO}_3^{=}$ result in low concentrations of Ca^{++} and Mg^{++} . The details of the results were less expected. With the GD sand, the initial peaks in calcium and magnesium concentrations (fig. 8) occurred simultaneously with the surprising sodium and potassium results in the early part of the flood, i.e., when the NaCl front was at about 0.7 PV. A more controlled experiment might make it possible to discern what processes are taking place. That is, the core should be saturated with a brine of uniform composition prior to injection of the alkali slug.

Whatever caused the peaks is evidently tapering off for half a pore volume prior to alkalinity breakthrough. In figure 9, the early part of the flood with LH sand gave smoother profiles. At 0.67 PV, the measured alkalinity was 0.0100 (table 13). Using the parameters for the carbonate reactions and the solubility product for CaCO_3 (K_{CALC} in table 15), we calculate

<u>pH</u>	<u>[CO₃⁼]</u>	<u>Equilibrium [Ca⁺⁺]</u>
6.5	1 X 10 ⁻⁵	2 X 10 ⁻⁴
7.0	5 X 10 ⁻⁵	6 X 10 ⁻⁵
8.0	5 X 10 ⁻³	6 X 10 ⁻⁶

The measured calcium concentration was 2.8×10^{-3} (fig. 9). This shows that for any reasonable guess at the effluent pH, the alkalinity and calcium concentration at this stage were not compatible for equilibrium. This confirms the previous observations about persistent super-saturation.

Silicon and Aluminum

For the GD sand with NaOH, comparison of figures 1, 4, 8, and 10 shows the following sequence of events:

1. 1.5 PV - alkalinity and sodium concentration rise rapidly; silicon and aluminum first appear.
2. 1.5 - 2.0 PV - alkalinity, sodium, and silicon go through maxima; aluminum rises rapidly.
3. 2.0 - 2.5 PV - alkalinity and sodium decline; silicon remains at a steady low concentration; aluminum is at a high plateau.
4. 2.5 - 3.0 PV - aluminum declines to zero; silicon rises rapidly; alkalinity and sodium rise after minima.
5. 3.5 PV on - alkalinity, sodium, and silicon remain fairly steady. Alkalinity and sodium are below the maximum (smaller than injected concentration).

The following processes can account for the observations, but of course are only speculations:

1. Breakthrough of NaOH.
2. Clays being dissolved.
3. A silica-rich mineral precipitates from super-saturated solution; rapid consumption of alkalinity and sodium compensates for the delay in the start of precipitation. The delay might be associated with a lag in nucleation.
4. Precipitation of a second mineral with higher aluminum content reduces dissolved aluminum and permits buildup of dissolved silicon.
5. Steady state between clay dissolution and new mineral formation, such that aluminum is precipitated as fast as it is dissolved.

With the LH sand and Na_2CO_3 , steady-state conditions were attained almost immediately (table 14). The effluent contained a low concentration of silicon and virtually no aluminum. Simple dissolution of quartz would not cause the reduction in alkalinity observed (fig. 2A). Possibly this is due to precipitation of divalent carbonates, which would account for the lack of sodium consumption (fig. 5). Some light could be shed on the process occurring during flow tests by examining the mineral to identify changes in composition after various times of exposure to alkali.

Comparison of Bottle and Slim Tube Tests

With the LH sand and Na_2CO_3 there was little consumption of alkalinity in either bottle tests (fig. 7) or slim tube tests (figs. 2A and 5). Results from both show a small stoichiometric surplus of sodium. Further experiments would be necessary to confirm or refute the above conjecture about divalent carbonate precipitation. The silicon and aluminum production in the LH sand - Na_2CO_3 bottle test (fig. 12) was qualitatively similar to that in the GD sand - NaOH slim tube test: there was an early maximum in aluminum concentration, accompanied by a level concentration of silicon; afterward the aluminum declined to virtually zero, and the silicon climbed to a high plateau. This suggests that similar chemical processes were taking place.

The GD sand - NaOH bottle test (fig. 11) gave no regions that were level in silicon concentration, at either a high or a low level. However, the aluminum pulse was complete in about 30 hr for both bottle and slim tube tests (reckoning time after alkaline breakthrough in the flow experiments). In each case, the aluminum concentration peaked at roughly 0.01 mol/kg. The silicon production was quantitatively different for bottle and slim tube tests, at least for the LH sand. The data are summarized here for ready reference:

<u>Sand/alkali</u>	<u>Silicon peak, mol/kg</u>		<u>initial pH</u>	<u>Final pH</u>	
	<u>Bottle</u>	<u>Tube</u>		<u>Bottle</u>	<u>Tube</u>
GD/NaOH	>0.2 ^{F11}	0.32 ^{F10}	13.5 ^{T12}	12.81 ^{T5}	-
LH/Na ₂ CO ₃	0.0039 ^{F12}	0.0003 ^{T14}	11.35 ^{T13}	10.66 ^{T10}	10.12 ^{T13}

(The superscripts T and F refer to table or figure numbers, respectively.)

It is interesting to see that the LH sand was more active in the bottle test, producing more silicon and aluminum. This may be associated with the observed higher final pH, which is predicted by the curves of figure 14. The absence of an early level region in silicon for the GD-NaOH bottle test remains unexplained. This casts doubts on the speculative mechanisms suggested by the slim tube tests. However, the overall conclusions drawn from the bottle tests were supported by the slim tube tests. In addition, the more-sensitive slim tube tests detected the fast reactions -- presumably ion exchange -- that were "invisible" in the bottle tests, and in hindsight suggested the possibility of carbonate precipitation in both types of tests. Mineral analysis would be informative in each case.

SUMMARY AND CONCLUSIONS

1. This work confirms that the adverse effect of mineral-alkali reactions decreases in the order hydroxide > silicate > carbonate.
2. Alkali consumption was severe in degree and duration for a high-clay sandstone and NaOH.

3. With a low-clay sandstone and Na_2CO_3 , consumption amounted to about 6% of injected alkalinity for a 1-PV slug. This is an encouraging result for the potential of low-pH alkaline flooding.
4. Fast consumption reactions, presumably ion exchange, are immediate. Slow reactions have an induction period.
5. Slow reactions result in the formation of new aluminosilicate minerals.
6. Carbonate systems exhibit slow or complex equilibria, with apparent supersaturation and values of pH that deviate from those calculated for the principal constituents.
7. These complex equilibria can be favorable or adverse. For realistic evaluation of alkaline flooding it should be tested under reservoir conditions of flow, temperature, and composition. In particular, in situ pH should be duplicated.
8. For a better understanding of the reaction processes between mineral and alkali, it is recommended that these studies be supplemented by conductivity measurements, pH titrations with definitive solutions and minerals, and an examination of mineral composition changes.
9. The agreement between bottle and slim-tube tests is imperfect, but controlled bottle tests are useful to predict behavior under flow conditions.
10. This work confirms that high-pH alkaline flooding is unlikely to be successful, but that there is considerable promise that a low-pH window can be found within which alkali-mineral reaction is reduced to an acceptable level, while the enhancement of oil mobilization is maintained at an acceptable level.

These results are in concert with conclusions of other investigators.

REFERENCES

1. Thornton, S. D. Adverse Effects of Mineral-Alkali Reactions in Alkaline Flooding. Final Report. Department of Energy Report No. NIPER-273. January 1988.
2. Patton, J. T. CO₂ Formation Damage Study, Final Report. U.S. Department of Energy Report No. DOE/MC/10865-13, July 1983.

TABLE 5. - Results of bottle test with Gu-Dao sandstone and 0.5 N NaOH solution at 60° C. Solid-liquid ratio is 0.2 kg sandstone/(kg solution)

Time, days	Alkalinity, equiv/(kg solution)	Concentration in solution			
		C _{Na} , mol/kg	C _{Si} , mol/kg	C _{Al} , mol/kg	C _K , mol/kg
0	0.481	0.478	0	0	--
1	--	0.483	0.00673	0.00230	--
5	--	0.478	0.0138	0.00519	--
9	--	0.483	0.0182	0.00585	--
19	--	0.478	0.0350	0.00648	--
37	--	0.461	0.0520	0.00052	--
63	--	0.435	0.0954	0.00026	--
100	0.411	0.448	0.133	0.00002	0.00079
135	0.410	0.439	0.172	0.00002	0.00082
170	¹ 0.404	0.426	0.193	0.00001	0.00082

¹Final pH was 12.81 at atmospheric conditions.

TABLE 6. - Results of bottle test with Gu-Dao sandstone and 0.5 N Na₂SiO₃ solution at 60° C. Solid-liquid ratio is 0.2 kg sandstone/(kg solution)

Time, days	Alkalinity, equiv/(kg solution)	Concentration in solution			
		C _{Na} , mol/kg	C _{Si} , mol/kg	C _{Al} , mol/kg	C _K , mol/kg
0	0.495	--	--	--	--
1	--	0.483	0.270	0.00006	--
5	--	0.474	0.269	0.00011	--
9	--	0.474	0.259	0.00023	--
19	--	0.465	0.269	0.00004	--
37	--	0.457	0.286	0.00004	--
63	--	0.457	0.307	0.00003	--
100	0.432	0.452	0.325	0.00002	0.00044
135	0.427	0.457	0.325	0.00002	0.00049
170	¹ 0.422	0.413	0.359	0.00002	0.00049

¹Final pH was 12.57 at atmospheric conditions.

TABLE 7. - Results of bottle test with Gu-Dao sandstone and 0.5 N Na₂CO₃ solution at 60° C. Solid-liquid ratio is 0.2 kg sandstone/(kg solution)

Time, days	Alkalinity, equiv/(kg solution)	Concentration in solution			
		C _{Na} , mol/kg	C _{Si} , mol/kg	C _{Al} , mol/kg	C _K , mol/kg
0	0.504	--	--	--	--
1	--	0.504	0.00079	0.00017	--
5	--	0.509	0.00082	0.00018	--
9	--	0.522	0.00085	0.00015	--
19	--	0.513	0.00081	0.00017	--
37	--	0.509	0.00071	0.00024	--
63	--	0.509	0.00083	0.00038	--
100	0.478	0.513	0.00022	0.00023	0.00038
135	0.481	0.504	0.00026	0.00025	0.00033
170	¹ 0.478	0.496	0.00030	0.00031	0.00033

¹Final pH was 10.46 at atmospheric conditions.

TABLE 8. - Results of bottle test with Liao-He sandstone and 0.5 N NaOH solution at 60° C. Solid-liquid ratio is 0.2 kg sandstone/(kg solution)

Time, days	Alkalinity, equiv/(kg solution)	Concentration in solution			
		C _{Na} , mol/kg	C _{Si} , mol/kg	C _{Al} , mol/kg	C _K , mol/kg
0	0.481	0.478	0	0	--
1	--	0.486	0.00434	0.00100	--
5	--	0.486	0.00854	0.00304	--
9	--	0.500	0.0117	0.00385	--
19	--	0.478	0.0160	0.00433	--
37	--	0.483	0.0222	0.00407	--
63	--	0.483	0.0270	0.00281	--
100	0.456	0.491	0.0466	0.00012	0.00107
135	0.457	0.482	0.0954	0.00003	0.00130
170	¹ 0.454	0.478	0.131	0.00002	0.00133

¹Final pH was 12.69 at atmospheric conditions.

TABLE 9. - Results of bottle test with Liao-He sandstone and 0.5 N Na_2SiO_3 solution at 60° C. Solid-liquid ratio is 0.2 kg sandstone/(kg solution)

Time, days	Alkalinity, equiv/(kg solution)	Concentration in solution			
		C_{Na} , mol/kg	C_{Si} , mol/kg	C_{Al} , mol/kg	C_{K} , mol/kg
0	0.495	--	--	--	--
1	--	0.483	0.262	0.00003	--
5	--	0.478	0.264	0.00003	--
9	--	0.483	0.274	0.00005	--
19	--	0.483	0.278	0.00004	--
37	--	0.483	0.296	0.00005	--
63	--	0.491	0.316	0.00004	--
100	0.479	0.496	0.352	0.00002	0.00051
135	0.473	0.491	0.344	0.00001	0.00059
170	¹ 0.472	0.478	0.340	0.00001	0.00064

¹Final pH was 12.52 at atmospheric conditions.

TABLE 10. - Results of bottle test with Liao-He sandstone and 0.5 N Na_2CO_3 solution at 60° C. Solid-liquid ratio is 0.2 kg sandstone/(kg solution)

Time, days	Alkalinity, equiv/(kg solution)	Concentration in solution			
		C_{Na} , mol/kg	C_{Si} , mol/kg	C_{Al} , mol/kg	C_{K} , mol/kg
0	0.504	--	--	--	--
1	-	(0.583)	0.00039	0.00014	--
5	--	0.526	0.00040	0.00005	--
9	--	0.509	0.00044	0.00004	--
19	--	0.504	0.00069	0.00001	--
37	--	0.517	0.00126	0	--
63	--	0.513	0.00206	0	--
100	0.506	0.539	0.00377	0	0.00043
135	0.515	0.535	0.00370	0	0.00041
170	¹ 0.522	0.539	0.00391	0	0.00041

¹Final pH was 10.66 at atmospheric conditions.

TABLE 11. - Consumption of alkali in slim-tube experiments

Experiment	Type of consumption	Range of pore volumes injected	Consumption of alkali, equiv/(kg sandstone)
Gu-Dao/NaOH	Fast reactions	1.0 - 2.0	0.055
Gu-Dao/NaOH	Slow reactions	2.0 - 6.3	0.097
Liao-He/Na ₂ CO ₃	Fast reactions	1.0 - 1.4	0.0055
Liao-He/Na ₂ CO ₃	Slow reactions	1.4 - 2.9	0.0038

TABLE 12. - Effluent profile for alkalinity in the slim tube experiment with Gu-Dao sandstone and 0.5 N NaOH solution. The pH of the injected solution was 13.50 at atmospheric conditions.

Pore volumes injected	Alkalinity of effluent, ¹ equiv/(kg solution)
0.25	0.0038
0.53	0.010
0.64	0.0082
0.74	0.011
0.86	0.011
0.98	0.021
1.14	0.084
1.32	0.110
1.50	0.294
1.70	0.424
1.94	0.434
2.30	0.361
2.54	0.311
3.04	0.385
4.06	0.403
5.19	0.411
6.26	0.423

¹Alkalinity of the influent solution was 0.481 equiv/(kg solution).

TABLE 13. - Effluent profile for alkalinity in the slim-tube experiment with Liao-He sandstone and 0.5 N Na₂CO₃ solution. The pH of the injected solution was 11.35 at atmospheric conditions.

Pore volumes injected	Alkalinity of effluent, ¹ equiv/(kg solution)	pH, at atmospheric conditions
0.15	0.0080	--
0.40	0.0094	--
0.67	0.0100	--
0.90	0.0126	--
1.01	0.178	--
1.10	0.419	--
1.21	0.473	--
1.33	0.476	--
1.53	0.477	10.07
1.76	0.491	10.11
2.08	0.489	10.10
2.50	0.494	10.10
2.83	0.496	10.12

¹Alkalinity of the influent solution was 0.499 equiv/(kg solution).

TABLE 14. - Silicon, aluminum, and potassium in the effluent from Liao-He sandstone during injection of 0.5 N Na₂CO₃ solution at 60° C

Pore volumes injected	Concentration in solution				
	C _{Mg} mol/kg	C _{Si} mol/kg	C _{Al} mol/kg	C _K mol/kg	C _{Ca} mol/kg
0.15	0.00099	0.00046	0	0.00192	0.00352
0.40	0.00111	0.00039	1x10 ⁻⁵	0.00115	0.00320
0.67	0.00120	0.00035	0	0.00130	0.00282
0.90	0.00116	0.00039	1x10 ⁻⁵	0.00069	0.00247
1.01	0.00040	0.00050	1x10 ⁻⁵	0.00046	5.8x10 ⁻⁵
1.10	4.5x10 ⁻⁵	0.00050	1x10 ⁻⁵	0.00041	2.4 - 10 ⁻⁵
1.21	8.6x10 ⁻⁶	0.00039	1x10 ⁻⁵	0.00036	1.4 - 10 ⁻⁵
1.33	7.4x10 ⁻⁶	0.00033	2x10 ⁻⁵	0.00036	1.3 - 10 ⁻⁵
1.42	7.0x10 ⁻⁶	0.00031	1x10 ⁻⁵	0.00031	1.2 - 10 ⁻⁵
1.53	7.8x10 ⁻⁶	0.00028	1x10 ⁻⁵	0.00036	1.2 - 10 ⁻⁵
1.66	7.8x10 ⁻⁶	0.00028	1x10 ⁻⁵	0.00038	1.1 - 10 ⁻⁵
1.76	9.9 - 6	0.00026	1x10 ⁻⁵	0.00041	1.2 - 10 ⁻⁵
1.87	8.6 - 6	0.00026	2x10 ⁻⁵	0.00041	1.2 - 10 ⁻⁵
1.98	1.0 - 5	0.00027	1x10 ⁻⁵	0.00041	1.6 - 10 ⁻⁵
2.08	9.1 - 6	0.00023	1x10 ⁻⁵	0.00041	1.5 - 10 ⁻⁵
2.19	1.1 - 5	0.00027	1x10 ⁻⁵	0.00041	1.5 - 10 ⁻⁵
2.30	9.9 - 6	0.00023	1x10 ⁻⁵	0.00046	1.5 - 10 ⁻⁵
2.39	8.6 - 6	0.00026	1x10 ⁻⁵	0.00046	1.6 - 10 ⁻⁵
2.50	9.1 - 6	0.00023	0	0.00046	1.5 - 10 ⁻⁵
2.66	9.1 - 6	0.00023	1x10 ⁻⁵	0.00051	1.5 - 10 ⁻⁵
2.83	9.1 - 6	0.00022	1x10 ⁻⁵	0.00051	1.4 - 10 ⁻⁵

TABLE 15. - Parameters used in calculation of saturation indices for calcite and chrysotile - 60° C

Parameter	Value
K_w	$10^{-13.02} \text{ mol}^2 \text{ dm}^{-6}$
h_{aq}	$10^{-1.84} \text{ mol dm}^{-3} \text{ atm}^{-1}$
K_{CALC}	$10^{-8.76} \text{ mol}^2 \text{ dm}^{-6}$
K_{CHR}	$10^{-48.9} \text{ mol}^{11} \text{ dm}^{-33}$
A.....	$10^{-0.26}$
B.....	$10^{7.53}$
Q_1	$10^{-5.90} \text{ mol dm}^{-3}$
Q_2	$10^{-9.33} \text{ mol dm}^{-3}$
Q_{Si}	$10^{-3.76} \text{ dm}^3 \text{ mol}^{-1}$

For sources of data, see reference 1.

TABLE 18. - Parameters used for calculation of carbon speciation. Conditions are: ionic strength = 0.5 mol dm^{-3} and temperature = 50° C

Parameter	Value
Q_1	$1.3 \times 10^{-6} \text{ mol dm}^{-3}$
Q_2	$4.2 \times 10^{-10} \text{ mol dm}^{-3}$
h_{aq}	$0.0179 \text{ mol dm}^{-3} \text{ atm}^{-1}$
h_{oleic}	$0.054 \text{ mol dm}^{-3} \text{ atm}^{-1}$

For sources of data, see reference 1.

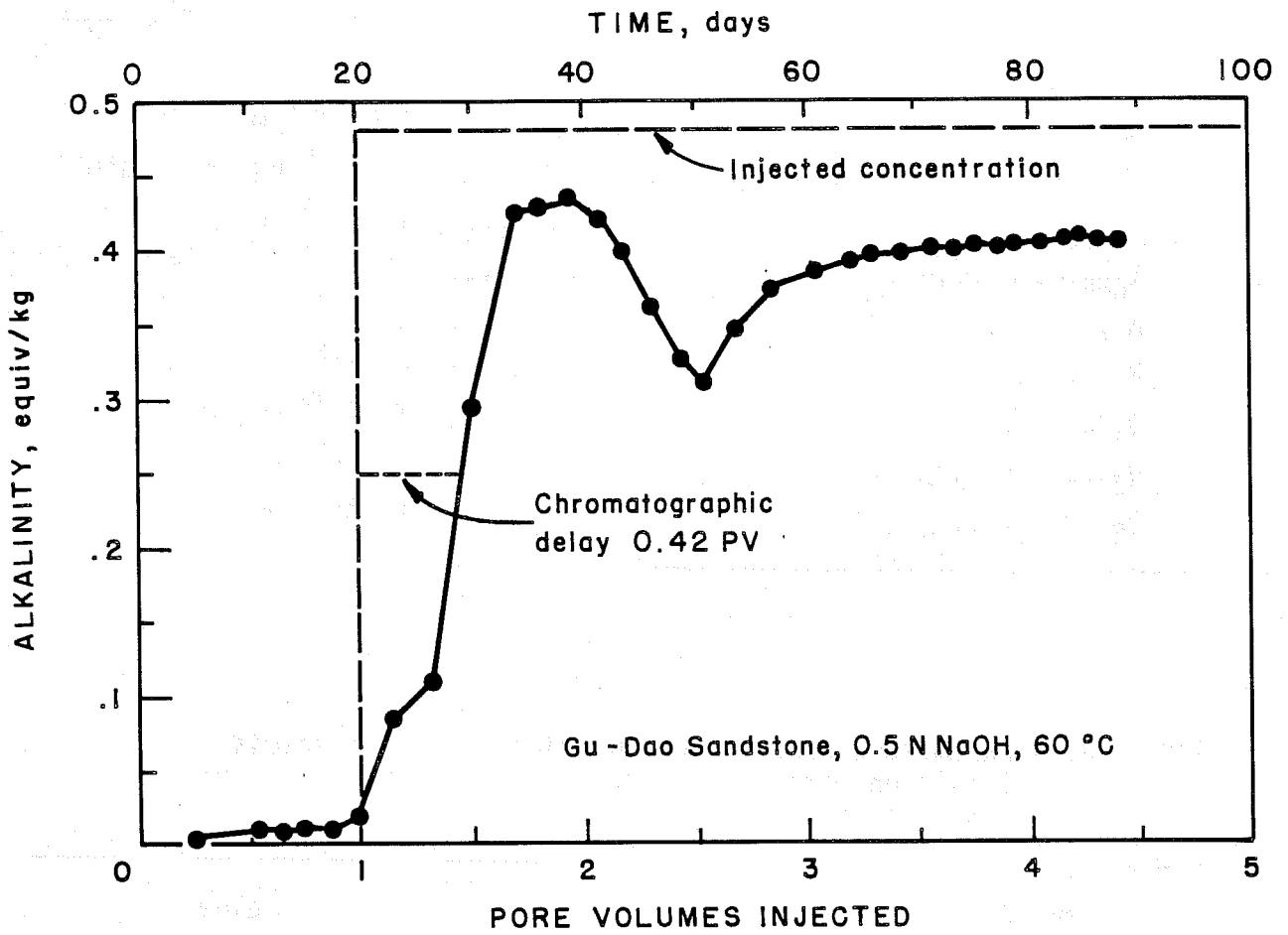


FIGURE 1. - Effluent profile for alkalinity in the Gu-Dao/NaOH slim-tube experiment.

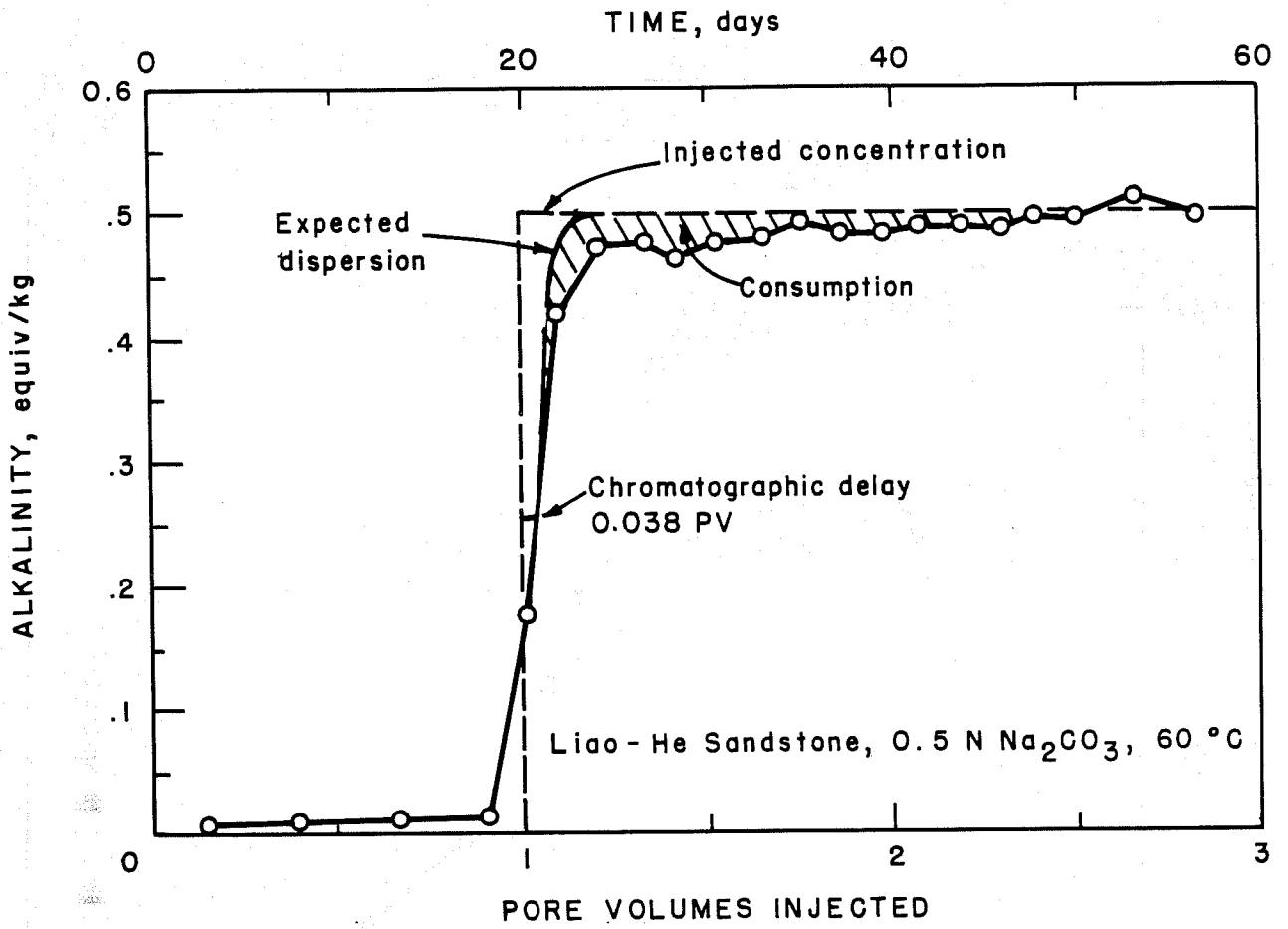


FIGURE 2A. - Effluent profile for alkalinity in the Liao-He/ Na_2CO_3 slim-tube experiment.

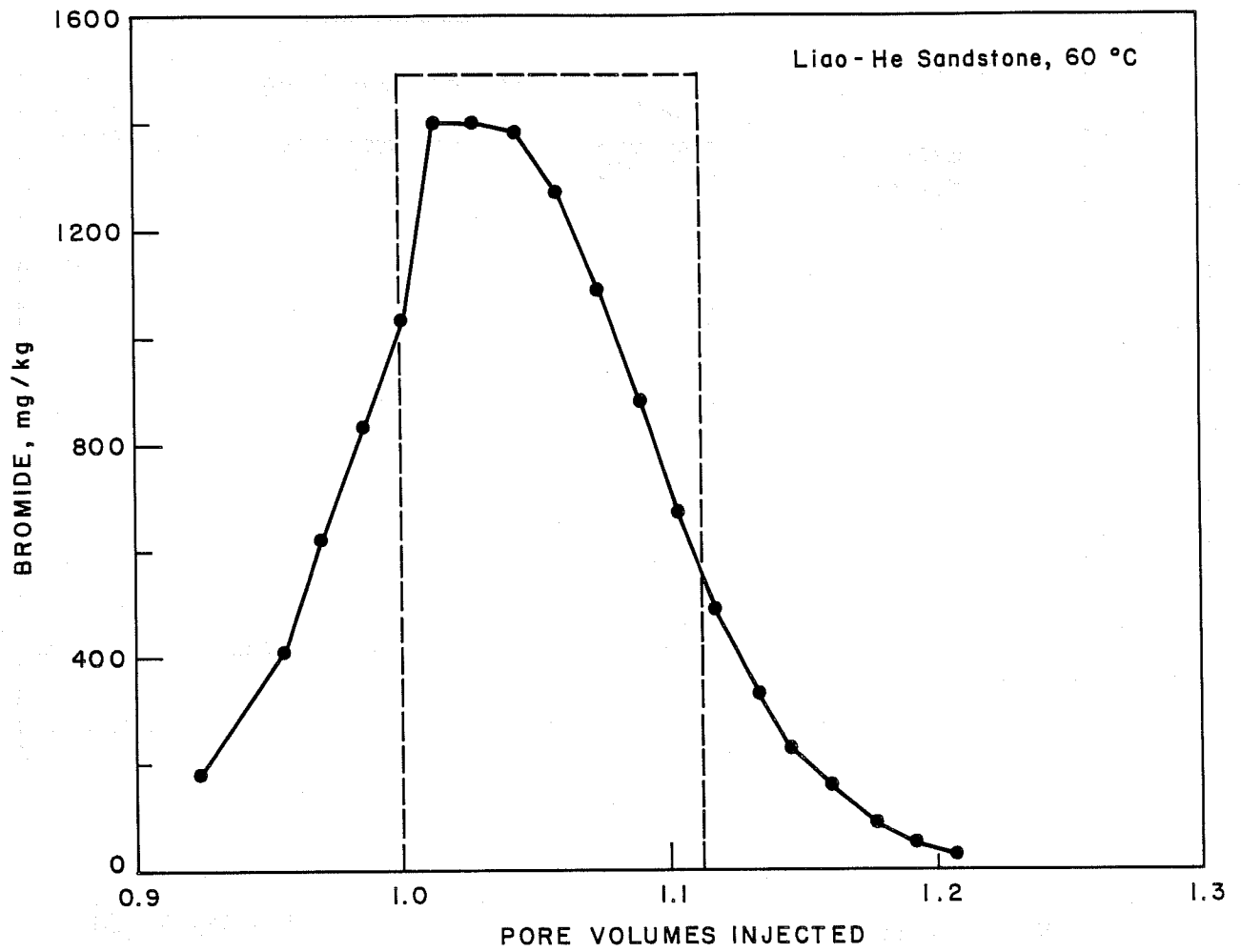


FIGURE 3. - Effluent profile for the tracer, bromide ion, in the Liao-He/ Na_2CO_3 slim-tube experiment.

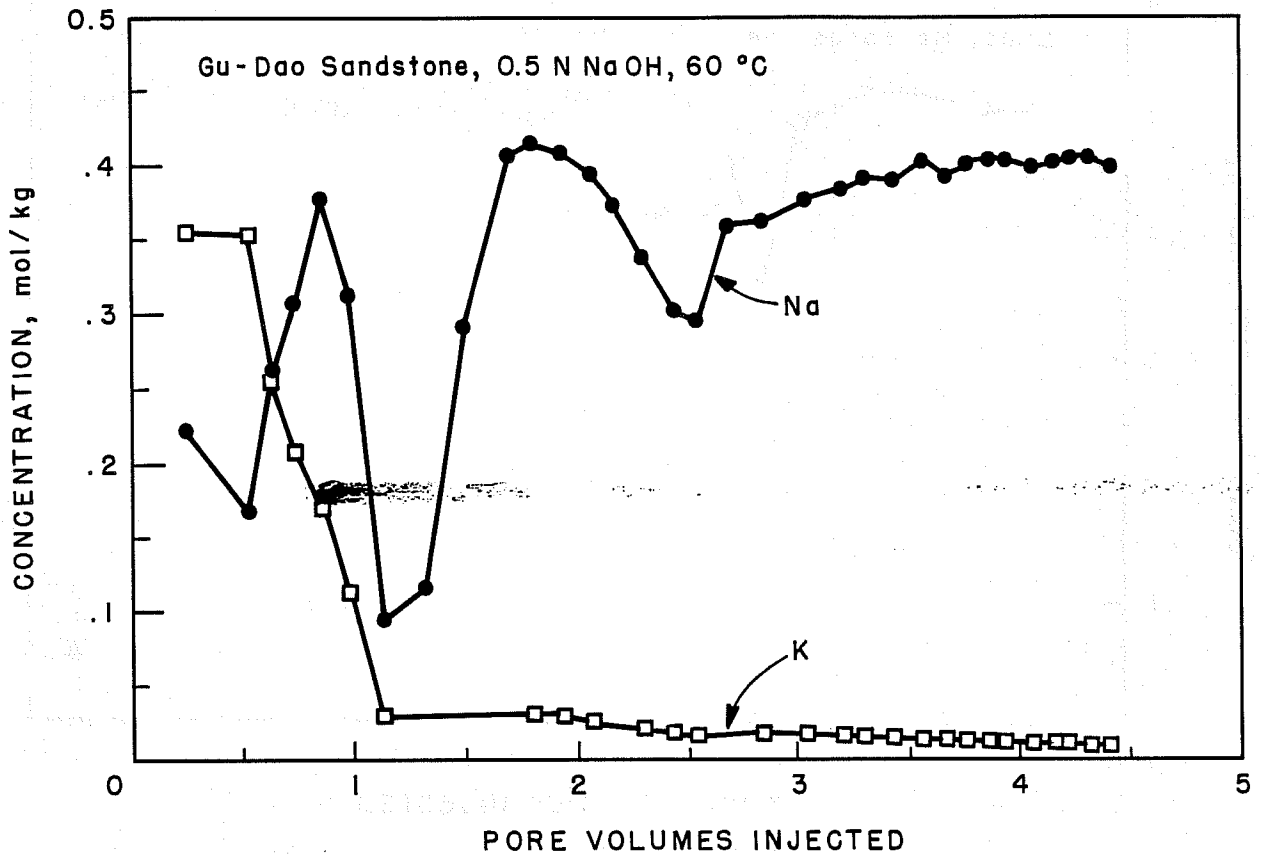


FIGURE 4. - Effluent profiles for sodium (Na) and potassium (K) in the Gu-Dao/NaOH slim-tube experiment.

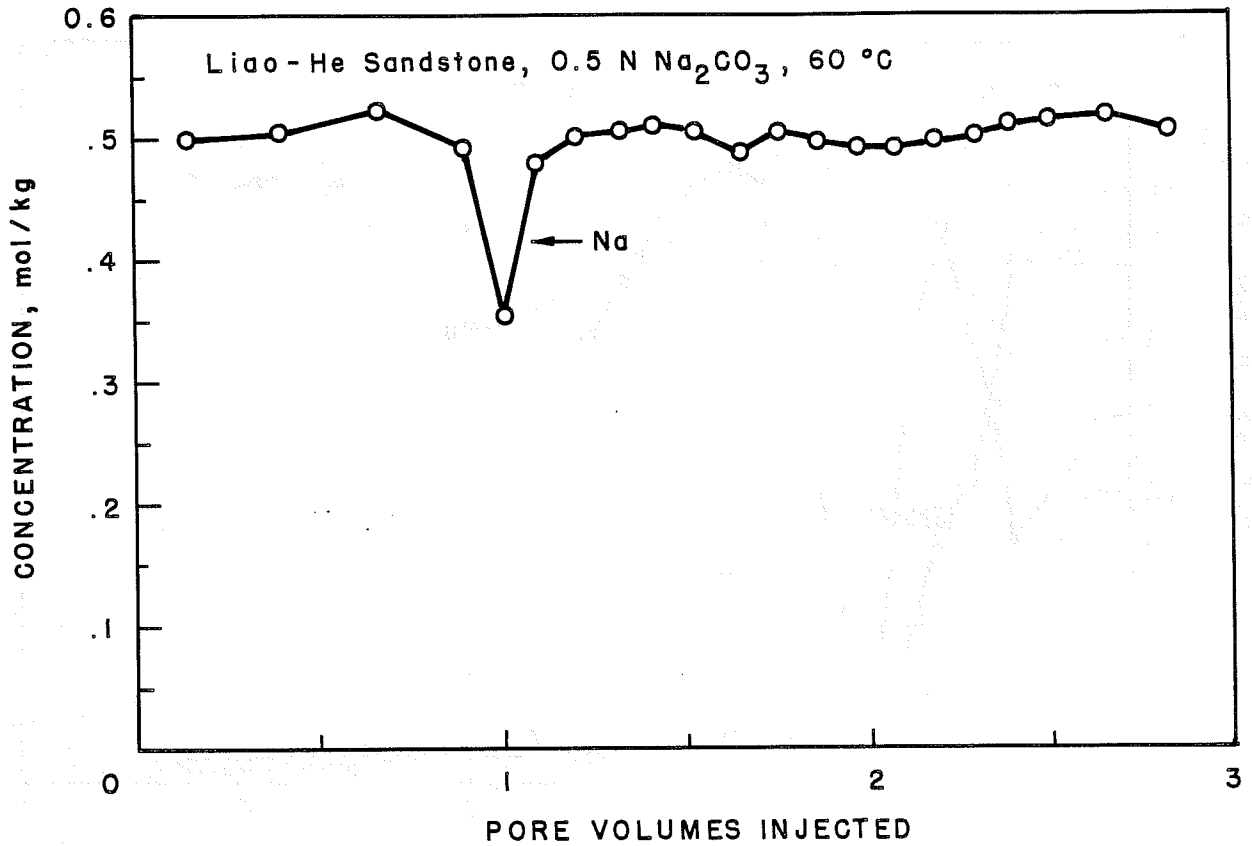


FIGURE 5. - Effluent profile for sodium (Na) in the Liao-He/ Na_2CO_3 slim-tube experiment.

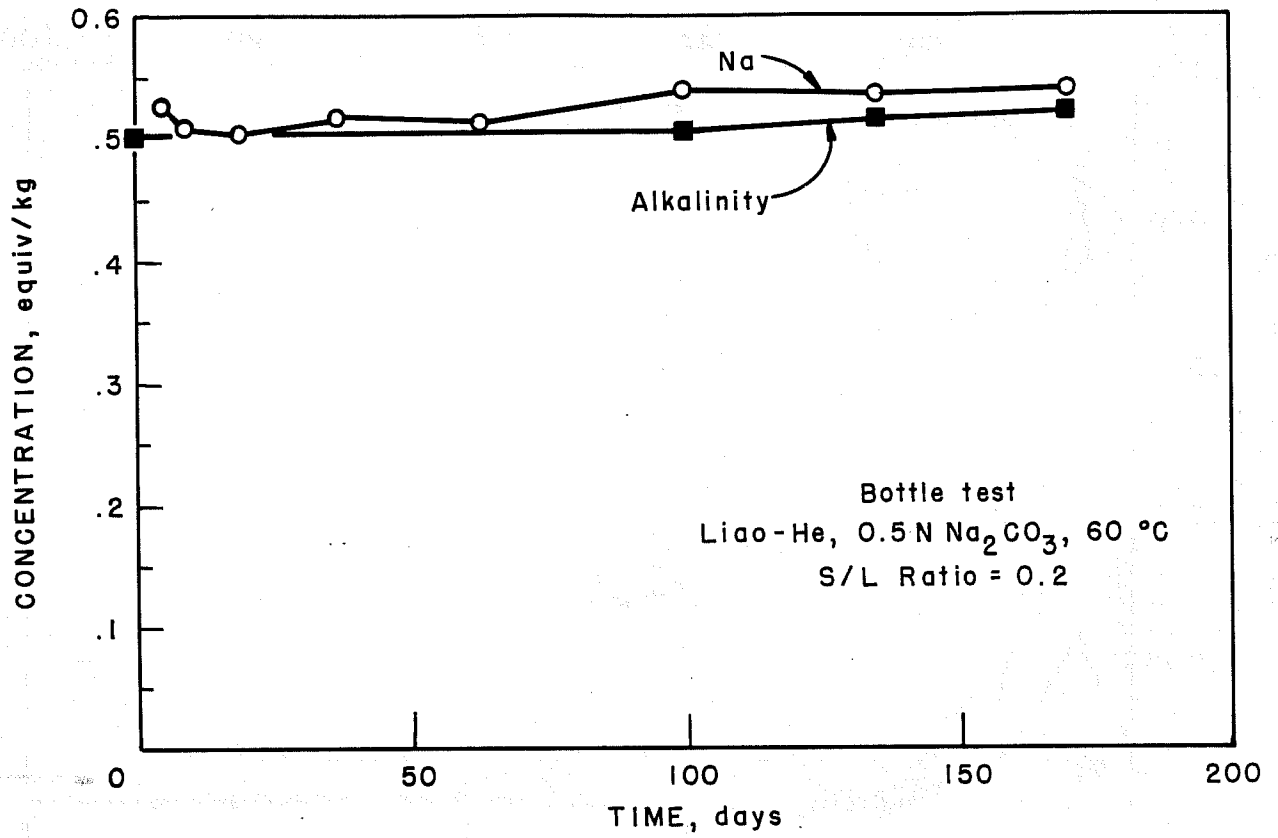


FIGURE 7. - Concentration of sodium (Na) and alkalinity versus time in the Liao-He/ Na_2CO_3 bottle test.

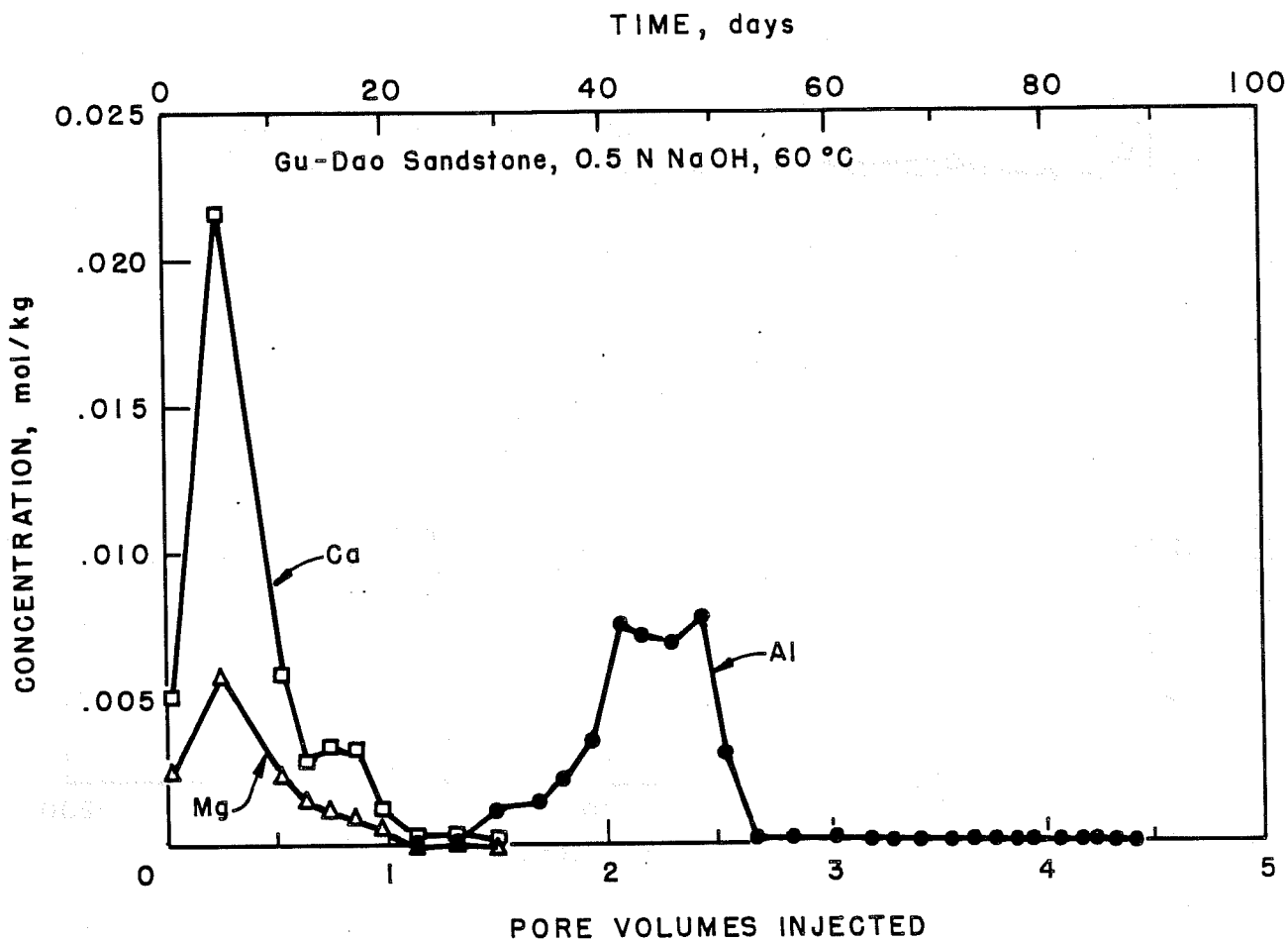


FIGURE 8. - Effluent profiles for calcium (Ca), magnesium (Mg), and aluminate ion (Al) in the Gu-Dao-NaOH slim-tube experiment.

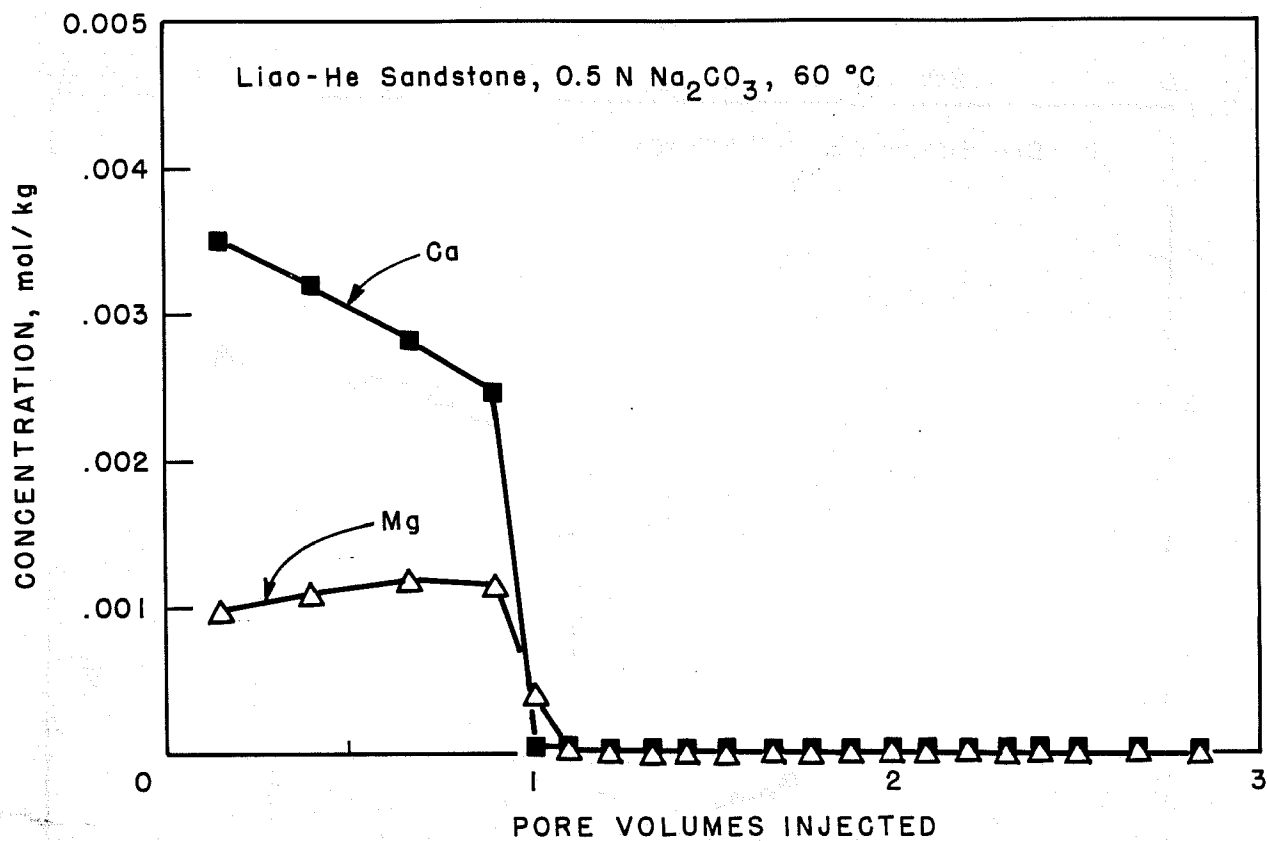


FIGURE 9. - Effluent profiles for calcium (Ca) and magnesium (Mg) in the Liao-He/Na₂CO₃ slim-tube experiment.

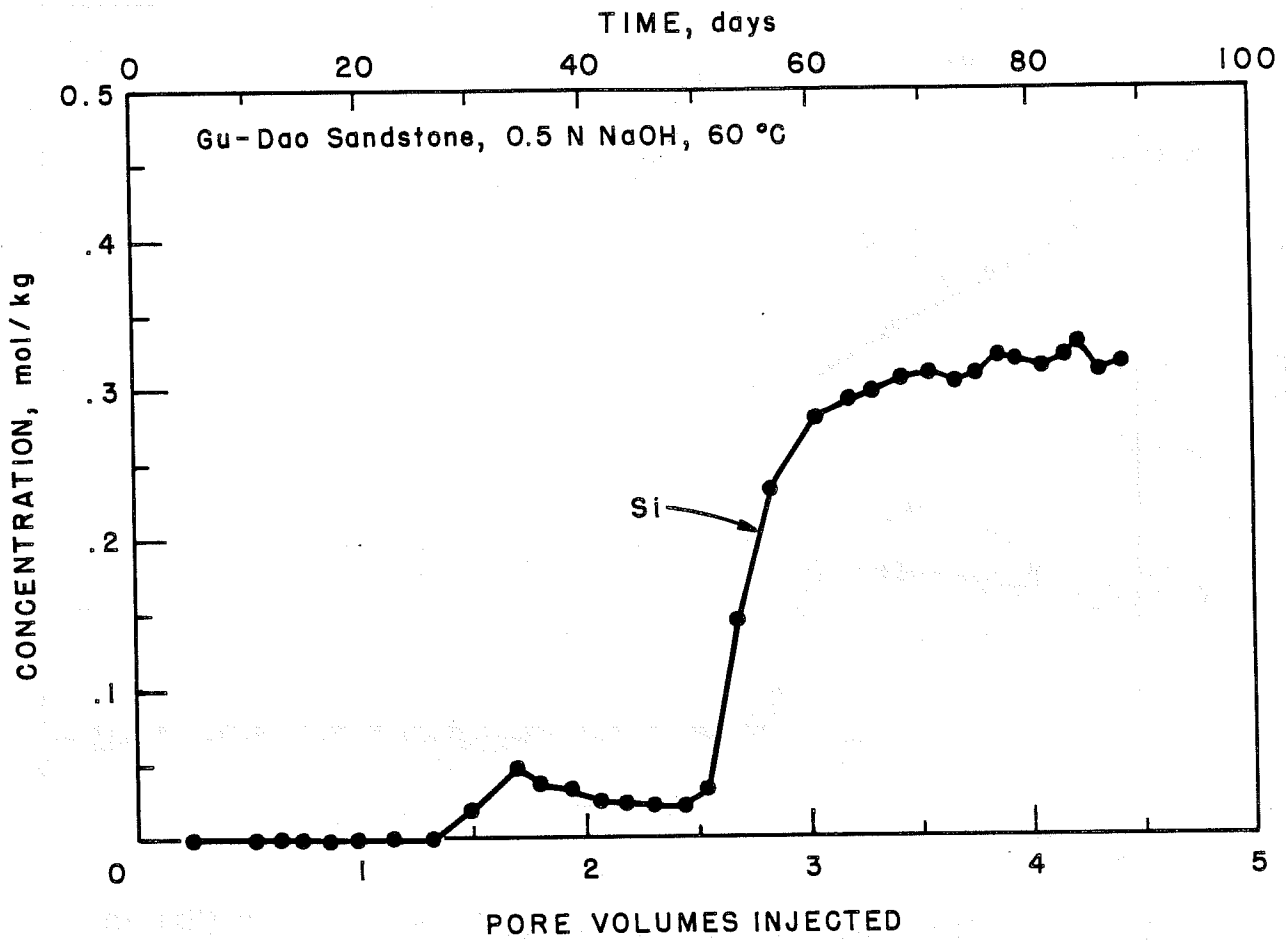


FIGURE 10. - Effluent profile for silicate ion (Si) in the Gu-Dao/NaOH slim-tube experiment.

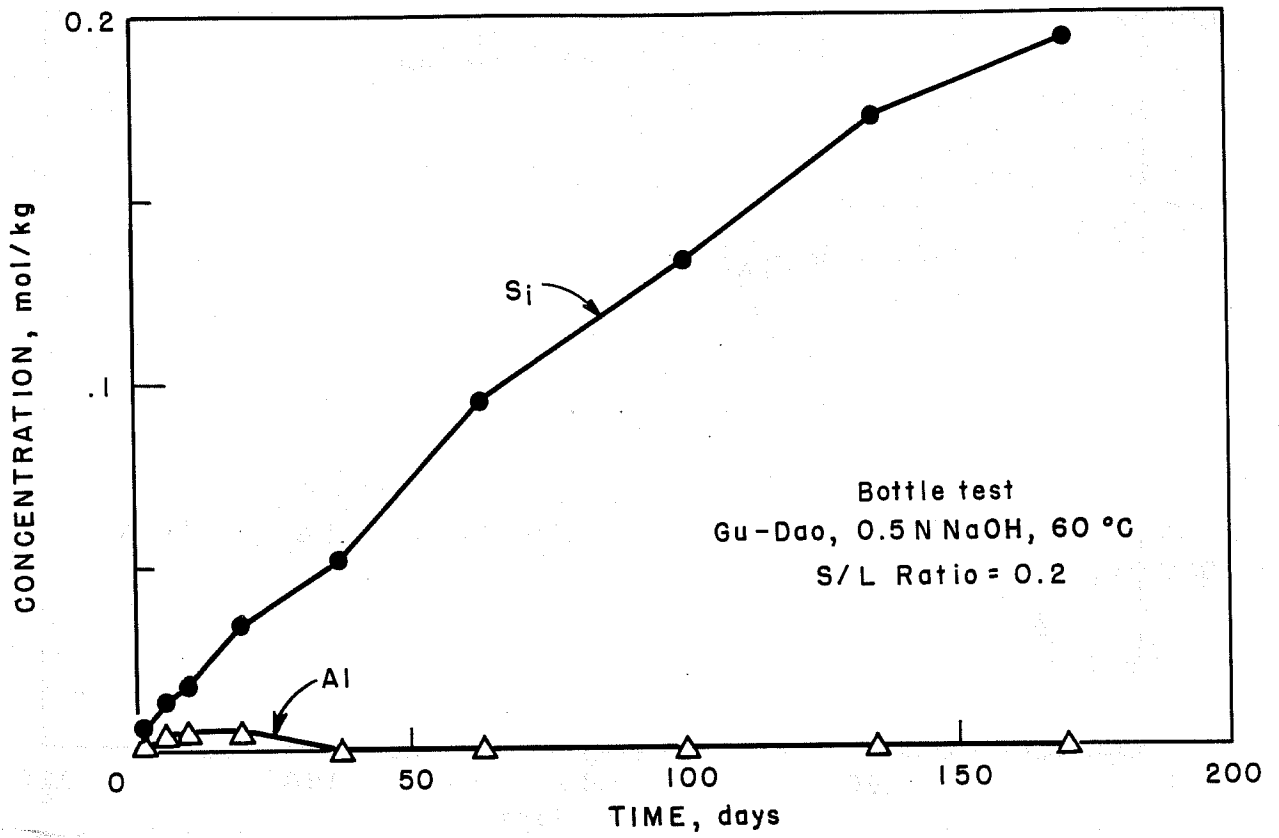


FIGURE 11. - Concentrations of silicate ion (Si) and aluminate ion (Al) versus time in the Gu-Dao/NaOH bottle test.

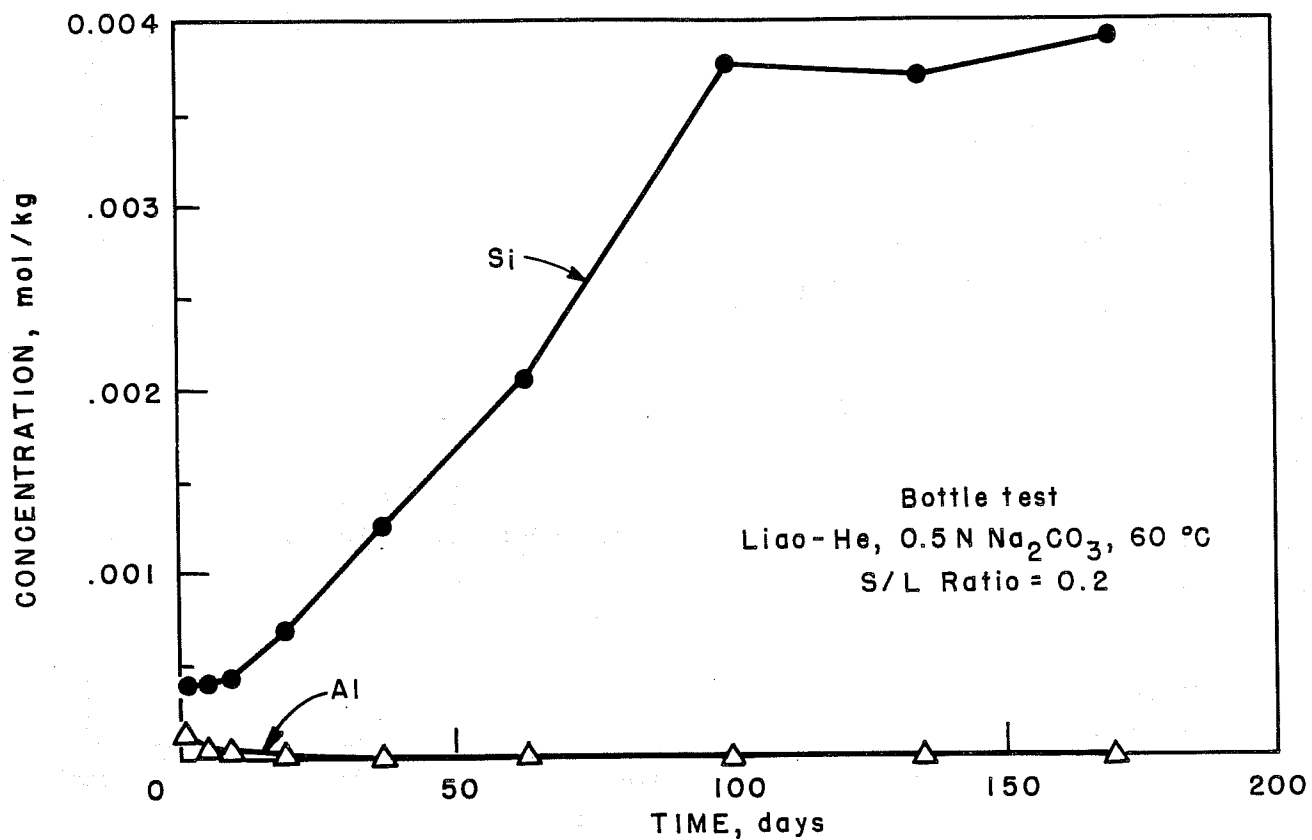


FIGURE 12. - Concentrations of silicate ion (Si) and aluminate ion (Al) versus time in the Liao-He/Na₂CO₃ bottle test.

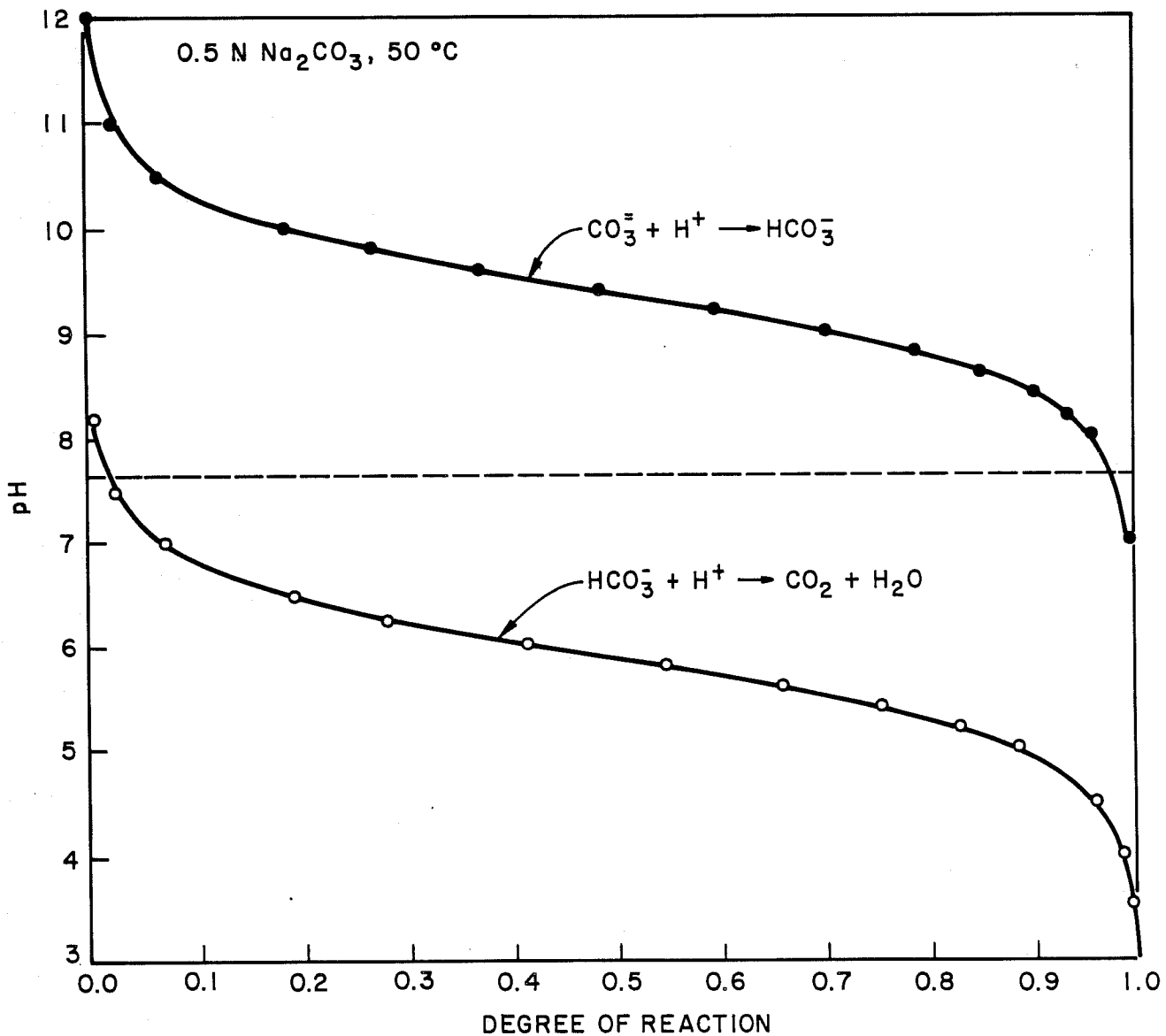


FIGURE 14A. - Calculated pH values for neutralization of carbonate and bicarbonate solutions. Dashed line shows pH value for symmetrical disproportionation of bicarbonate ion.

